BLAST RESPONSE LIMITS FOR LOAD-BEARING PRESTRESSED CONCRETE PANELS

Thomas J. Mander, P.E., Baker Engineering and Risk Consultants, Inc., San Antonio, TX
Michael J. Lowak, Baker Engineering and Risk Consultants, Inc., San Antonio, TX
Michael A. Polcyn, Baker Engineering and Risk Consultants, Inc., San Antonio, TX

ABSTRACT

Buildings susceptible to blast load threats are required to undergo deformations much larger than those expected for conventional loading. The deformation of individual building components is typically calculated using non-linear single degree of freedom (SDOF) analyses. These deformations are compared to published response limits to quantify the expected level of blast damage. Currently, no such limits exist for load-bearing prestressed concrete wall panels.

This paper presents design response limits for load-bearing prestressed concrete wall panels, based on a series of full-scale shock tube tests and dynamic analysis. The panels tested included 6-inch thick solid prestressed concrete panels and prestressed concrete insulated panels with 3-inch thick wythes separated with 2 inches of rigid insulation. Static axial loads were sustained on the top of the panels in the dynamic shock tube tests, ranging from 5 and 10 percent of the gross static axial capacity of each wall. Test results are summarized, along with SDOF analytical comparisons, which were used to develop load-bearing prestressed concrete blast response criteria.

Keywords: Blast, Shock Tube, Prestressed Concrete Panels, Load-bearing, Response Criteria, Dynamic Analysis

INTRODUCTION

Precast concrete walls are an effective means of construction for government and industrial buildings. Reducing onsite construction can create cost and time savings to the building owner. Construction time can be further expedited if the walls are load-bearing (LB) members. In addition to expedited construction, prestressed concrete walls benefit from initial pre-compression, which allows thinner walls compared to a conventionally reinforced concrete wall to satisfy serviceability requirements. Prestressing strands also provide re-centering forces when a wall is displaced laterally, reducing the permanent displacements compared to a reinforced concrete wall.

In spite of these attributes, prestressed LB wall systems have infrequent use in blast settings, owed to the lack of research in this area. Blast analysis and design requires established response criteria to which structural components are designed. Currently, such criteria does not exist for LB prestressed concrete walls. This paper presents Single-Degree-of-Freedom (SDOF) response criteria that will allow the expanded use of LB structural panels in blast-resistant construction.

Criteria were developed through analysis and validated with a series of shock tube tests, performed on full scale LB panels. Panel construction included solid prestressed panels and prestressed insulated panels. LB panels supported a concentric axial load with a magnitude expressed as an equivalent uniform stress that is a fraction of the specified concrete strength of 5 percent and 10 percent of each panel ($0.05\,f'_cA_g$ and $0.10f'_cA_g$). This load conservatively represents a combination of static (dead and live) loads and dynamic reactions from supporting components (such as roof members).

RESPONSE CRITERIA FOR BLAST DESIGN

The development of blast response criteria is significantly different from the development of standards for conventional design loads. Blast performance criteria assumes a single loading event, allowing structural damage. The limit of extent of the damage is related to the level of protection the structure is required to provide to the building occupants. Unlike seismic performance criteria, blast performance criteria are based on the performance of the structural component through only one or two cycles. Therefore, a loss of capacity may be tolerable so long as the damaged element can still carry the anticipated loads that will be present immediately after the event.

Blast analysis and design of such panels are most commonly performed at a component level using SDOF methods. The peak deflection and corresponding support rotation from the SDOF analysis are of key importance, and are compared to prescribed limits to satisfy a level of component damage. Limiting values are in terms of support rotation, θ, and displacement ductility, μ. The calculation of support rotation from deflection uses the idealization shown in Figure 1, which assumes development of a plastic hinge for a simply-supported beam or panel at mid-span. The displacement ductility is calculated using Equation (1), as the ratio of

peak SDOF displacement d_{max} to yield displacement, d_y.

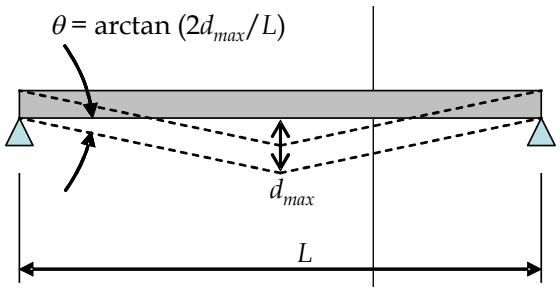

Figure 1. Definition of Support Rotation as Function of Maximum Displacement

Equation (1)

ASCE 59-11ASCE 59-11, Blast Protection of Buildings, Published by the American Society of Engineers (ASCE), Reston, VA, 2011. uses response limits from the U.S. Army Corps of Engineers (USACE) Protective Design Center (PDC) response criteria for SDOF componentsPDC TR-06-01, "Methodology Manual for the Single-Degree-of-Freedom Blast Effects Design Spreadsheets (SBEDS)," U.S. Army Corps of Engineers (USACE), Protective Design Center (PDC) Technical Report 06-01, Sep. 2006.·PDC TR-06-08, "Single Degree of Freedom Response Limits for Antiterrorism Design," USACE PDC Technical Report 06-08, Jan. 2008.. These limits were developed for Department of Defense (DoD) facilities designed against high explosive terrorist threats. Four Levels of Protection (LOP) are defined as: High (HLOP), Medium (MLOP), Low (LLOP) and Very Low (VLLOP). These LOPs respectively correspond to expected element damage denoted by the USACE as Superficial, Moderate, Heavy, and Hazardous. Qualitative damage expectations for each of these four limit states, per PDC TR-06-08, are provided in Table 1. Currently, quantitative response criteria for LB prestressed concrete walls are not published, motivating the need for the research presented herein. Existing response limits for non-load-bearing (NLB) panels are listed in Table 2. The prestressing index, ω_p, is calculated using Equation (2).

Equation (2)

Table 1. Qualitative Response Limits for All Structural Components (from PDC TR-06-08)

PDC TR-06-08 Damage Level	Component Consequence
B1 (HLOP)	Superficial damage. Component has no visible damage.
B2 (MLOP)	Moderate damage. Component has some permanent deflection. It is generally repairable, if necessary, although replacement may be more economical and aesthetic.
B3 (LLOP)	Heavy Damage. Component has not failed, but it has significant permanent deflections, causing it to be irreparable.

B4 (VLLOP)	Hazardous Failure. Component has failed, and debris velocities range from insignificant to very significant.
> B4	Blowout. Component is overwhelmed by the blast load causing debris with significant velocities.

Table 2. Non-Load-Bearing Prestressed Concrete Response Limits (from PDC TR-06-08)

Reinforcement Index	Superficial Damage		Moderate Damage		Heavy Damage		Hazardous Failure	
	μ	θ	μ	θ	μ	θ	μ	θ
$\omega_p > 0.30$	0.7	-	0.8	-	0.9	-	1	
$0.15 \le \omega_p \le 0.30$ or members with $\omega_p \le 0.15$ and no shear reinforcement	0.8	-		1°		1.5°		2°
$\omega_p \le 0.15$ with shear reinforcement	1	-	-	1°	-	2°	-	3°

EXPERIMENTAL STUDY

A total of eighteen different precast, prestressed panel specimens were tested in the BakerRisk shock tube. The overall objective of the test program was to subject various precast, prestressed wall panels to Moderate (M) and Heavy (H) damage levels.
describes the panel specimens used for the shock tube test matrix. Some panels were tested multiple times to determine different damage thresholds. A total of 30 shock tube tests were accomplished.

All specimens were full-scale 4-foot wide panels spanning 16 feet between supports, representative of typical interstory building heights. Panels were cast by a certified PCI precaster. Insulated panels were constructed with a bond breaker between the concrete wythes and insulation. This was purposely done to conservatively simulate potential long term bond loss or poor cohesion (oil on foam) in casting. Concrete with a compressive strength of 5000 psi was specified for all panel specimens. At the time of shock tube testing, compression strengths were measured. The average compression strength of three 6-inch × 12-inch concrete cylinders is reported in
. Note that the axial load magnitude is in terms of the specified 5000 psi compressive strength.

Figure 2 shows the BakerRisk shock tube with a single panel specimen mounted at the end of the 16-foot high × 10-foot wide expansion section. The 3-foot open width on the sides of the panel specimen were covered with steel plate bolted to the shock tube frame, and stiffened along the free edge with vertical hollow structural sections to reduce blast clearing. Blast clearing occurs when an incident blast wave strikes a wall of finite size in a normal orientation, and rarefaction waves are created at the edges of the wall. These rarefaction waves sweep inward from the sides, resulting in reduced overpressures and overall reduction in applied impulse.Geng, J., Mander, T.J., and Baker, Q.A., “Blast Wave Clearing Behavior

for Positive and Negative Phases," Journal of Loss Prevention in the Process Industries, available online 24 October 2014.

A slight (¼-inch) gap was left between the vertical edges of the panels to prevent any form of contact to the test frame under dynamic response. Figure 2(a) shows a NLB panel prior to testing, and Figure 2(b) shows a LB specimen with the axial load apparatus at the top of the wall. The axial load applicator is the first known of its kind. Traditionally, researchers use hydraulic actuators, but these do not respond fast enough under dynamic loading to maintain a constant axial load. The apparatus shown utilizes air bladders that are contained within a fixed steel chamber, which applies force to vertical steel pistons. The pistons apply load to a spreader beam, in turn loading the top of the wall.

Table 3. Panel Specimens for Shock Tube Tests

Panel Type	Targeted Response	Axial Load	f'_c at test date (psi)	Panel Construction
Solid Prestressed	M and H	None	7200	6-inch thick panel with five 3/8-inch dia. Gr 270 strands at mid-depth (ω_p = 0.15) and WWR 6 × 6-D4 × D4 at mid-depth.
	M	$0.10f'_cA_g$	7200	
	H	$0.10f'_cA_g$	7200	
	M	$0.05f'_cA_g$	5200	
	H	$0.05f'_cA_g$	5200	
Prestressed Insulated – Fully Composite for Ultimate Strength	M and H	None	7000	3/2/3 panel, with three 3/8-inch dia. Gr 270 strands (ω_p = 0.04) and WWR 6 × 6-D4 × D4 mid-depth in each wythe. Two continuous P12G welded wire girders with 0 gauge (0.306 inch) top and bottom wire, 3 gauge diagonal (0.243 inch), 5.5 inch truss height.
	M	$0.10f'_cA_g$	7000	
	H	$0.10f'_cA_g$	7000	
	M	$0.05f'_cA_g$	7100	
	H	$0.05f'_cA_g$	7100	
Prestressed Insulated – Partially Composite for Ultimate Strength	M and H	None	6900	Truss girders spaced intermittently to equate to 60% of shear connectors provided for the fully composite design.
	M	$0.10f'_cA_g$	6900	
	H	$0.10f'_cA_g$	6900	
	M	$0.05f'_cA_g$	5200	
	H	$0.05f'_cA_g$	5200	

It is recognized that many load-bearing precast insulated panels are designed so the interior wythe supports conventional axial loads. This axial load is usually eccentric to the interior wythe, creating an outward bending moment. The moment counteracts the effect of blast overpressures that create bending inward on the structure. Hence it is conservative to apply an axial load concentrically to the panel. Additionally, in the case of continuous fully-composite panels that support more than one story, or for panels with solid concrete regions at the support for connection requirements, the exterior wythe will also carry axial load. The out-of-plane displacement of the panel from blast loading will cause compression on the exterior wythe, for a fully or partially composite panel, and the axial load is transferred to

this wythe through the shear connectors. Therefore, the axial load setup utilized in the test program is considered to be conservative for realistic loading conditions. The actual eccentricity of load can be considered in the analysis as demonstrated later in this paper.

(a) **Non-Load-Bearing Wall** (b) **Load-Bearing Wall**

Figure 2. Wall Specimens Mounted in Shock Tube

Connections were simple bearing connections to eliminate connection variability from the dynamic response. As is the case with shear tie connectors, various proprietary panel-to-superstructure connections exist in the precast industry. It was not deemed practical to consider different connections in this study, or to place bias on a single type of connector. In addition, a separate shock tube test program on conventionally reinforced precast non-load-bearing panels, with various precast connections, saw panel support rotations reach 12 degrees without observing connection failure.Lowak, M.J., and Montoya, J.R., "Shock Tube Testing of Precast Concrete Panels," Prepared for Protection Engineering Consultants, Inc., BakerRisk Project No. 01-03471-001-11, March, 2012. The connections were designed using LRFD, following the equations of the PCI Design Handbook.PCI Industry Handbook Committee, PCI Design Handbook – Precast and Prestressed Concrete, Seventh Edition, Chicago, Illinois, 2010. The design load demand was set equal to the reaction associated with the ultimate dynamic resistance of the panels. Precast test panel connections designed by this method only failed in one case out of 14 tests.

Displacements were measured using an accelerometer at panel mid-height. These measurements were confirmed by overlaying a semi-transparent photo of a ½-inch grid on the side-elevation high-speed (HS) video recordings for each panel. Additional HS and high-definition (HD) videos were taken from the front elevation. Photographs were taken before and after each test, and cracks were traced with markers to increase visibility in the photographs. Whenever possible, multiple (repeat) tests were conducted on the same panels after observing panel damage to maximize the amount of data produced from this research.

The experimental data for solid prestressed panels, fully composite panels, and partially (60%) composite panels are provided in Table 4, Table 5, and Table 6, respectively. The results are divided into panel type, rather than in test number order. Although only eighteen panel specimens were available, thirty shock tube tests were completed. Panels that were tested multiple times are indicated with an asterisk. The tables include peak pressure, applied impulse, peak mid-height displacement, Δ_{max}, peak support rotation, θ_{max}, residual mid-height displacement, $\Delta_{res,}$ residual support rotation, θ_{res}, and a qualitative description of damage

Table 4. Solid Prestressed Panel Shock Tube Test Results

Test	Axial (kips)	P (psig)	i (psi-ms)	Δ_{max} (inch)	θ_{max}	Δ_{res} (inch)	θ_{res}	Observed Damage
1	0	4.4	78	1.8	1.1°	0.2	0.12°	Hairline Cracking (Superficial)
2*	0	5.9	103	4.2	2.6°	0.4	0.25	Cracking & residual disp. (Moderate)
3*	0	5.9	112	5.9	3.6°	0.5	0.31°	Widespread Cracking (Heavy)
4*	0	7.2	146	Fails ~12	7.4°	-	-	Strand Fracture (Blowout)
10	144	6.0	114	2.3	1.4°	0.1	0.06°	Cracking & residual disp. (Moderate)
11*	144	6.6	127	3.1	1.9°	0.3	0.18°	Cracking & residual disp. (Moderate)
15	144	7.0	128	3.4	2.1°	0.44	0.27°	Cracking & residual disp. (Moderate)
16*	144	7.3	135	Fails ~5.5	3.4°	-	-	Mid-height comp. failure (Blowout)
21	88	6.4	105	2.6	1.6°	0.19	0.12°	Cracking & residual disp. (Moderate)
22	72	7.0	120	3.6	2.2°	0.25	0.15°	Cracking & residual disp. (Moderate)
27	72	5.9	105	2.75	1.7°	0.1	0.06°	Cracking & residual disp. (Moderate)
28*	72	7.1	122	3.9	2.4°	0.625	0.39°	Significant residual disp. (Heavy)

* Denotes previously tested specimen

Table 5. Fully Composite Prestressed Insulated Panel Shock Tube Test Results

Test	Axial (kips)	P (psig)	i (psi-ms)	Δ_{max} (inch)	θ_{max}	Δ_{res} (inch)	θ_{res}	Observed Damage
5	0	6.4	122	2.3	1.4°	0.8	0.5°	Cracking & residual disp. (Moderate)
6*	0	6.9	138	5.1	3.1°	1.5	0.9°	Prestress bond failure cracks (Heavy)
12	144	7.1	148	Fails ~ 7	4.3°	-	-	Mid-height strand fracture (Blowout)
17	144	4.5	75	1.3	0.8°	0	0°	No visible cracks (Superficial)
18*	144	5.6	93	1.9	1.2°	0.44	0.3°	Cracking & residual disp. (Moderate)
19*	144	6.4	115	3.3	2.0°	1.1	0.7°	Significant permanent disp. (Heavy)
23	72	7.2	130	2.0	1.2°	0.31	0.2°	Cracking & residual disp. (Moderate)
24	72	7.8	147	2.9	1.8°	0.75	0.5°	Significant residual disp. (Heavy)
29	72	8.7	168	3.9	2.4°	1.25	0.8°	Significant residual disp. (Heavy)

* Denotes previously tested specimen

Qualitative damage was defined in terms of visible damage. Superficial damage was set for panels with hairline cracking and no permanent displacement. Moderate damage included panels with cracks less than ¼-inch wide (typical acceptable width for epoxy injection repair) and maximum residual displacements less than $L/360$ for LB panels, where L is the panel span length. This residual displacement equates to a ½-inch out-of-plane mid-height displacement for the panels tested. It was selected based on the allowable PCI Design Handbook (Chapter 13.2.8) bowing tolerances, recognizing that Moderate damage implies a component could be re-used. Finally, Heavy damage was classified as visible damage

exceeding the Moderate threshold.

Table 6. Partially Composite Prestressed Insulated Panel Shock Tube Test Results

Test	Axial (kips)	P (psig)	i (psi-ms)	Δ_{max} (inch)	θ_{max}	Δ_{res} (inch)	θ_{res}	Observed Damage
7	0	4.2	79	1.5	0.9°	0.3	0.2°	Cracking & residual disp. (Moderate)
8*	0	6.4	125	4.3	2.6°	0.9	0.6°	Significant residual disp. (Heavy)
9*	0	7.1	150	7.0	4.3°	1.3	0.8°	Significant residual disp. (Heavy)
13	144	4.4	77	1.5	0.9°	0	0°	Hairline Cracking (Superficial)
14*	144	5.3	97	2.5	1.5°	0.5	0.3°	Cracking & residual disp. (Moderate)
20	144	6.8	123	3.3	2.0°	1.1	0.7°	Significant residual disp. (Heavy)
25	72	7.0	120	2.4	1.5°	0.4	0.2°	Cracking & residual disp. (Moderate)
26	72	7.9	144	3.2	2.0°	0.9	0.5°	Significant residual disp. (Heavy)
30	72	8.1	157	5.5	3.4°	2.0	1.2°	Cracking & large perm. def. (Heavy)

* Denotes previously tested specimen

SDOF ANALYSIS OF TEST DATA

Blast design guidelines specify that the ultimate (plastic) capacity of prestressed concrete sections be based upon static principles, albeit using assumed dynamic increase factors for concrete and conventional steel. An elastic-plastic resistance function is commonly employed in SDOF analyses for components responding in flexure. The peak dynamic deflection is of primary interest from an SDOF analysis, and is converted to an equivalent support rotation, using the equation shown earlier in Figure 1, and compared to quantitative criteria. This method does not account for the actual state of stress or strain in the concrete and reinforcement when the panel reaches its maximum deflection.

The SDOF method is based on a structural component behaving such that its response can be adequately modeled by quantifying a single variable (usually displacement). The component is converted into an equivalent mass-spring-damper system, from which the equation of motion is solved:

Equation (2)

where K_{LM} is the load-mass factor to convert the component into an equivalent SDOF system using the actual mass, m, resistance, R, and damping c. The blast load, $p(t)$, is the forcing function while the acceleration, , velocity, , and displacement, , are solved for using numerical integration. With the addition of axial load, Equation (2) can be modified to include an equivalent lateral force equivalent to the $P\Delta$ moment. Alternatively, the PΔ moment can be subtracted from the resistance function and accounted for in the $R(x)$ term. The former method was adopted in this study.

Equation (3)

where P is the axial load per unit width, e is the eccentricity of the load, and L is the span between lateral supports.

The state of the practice for simplified SDOF blast assessments is to utilize an elastic-perfectly-plastic resistance function. The ultimate resistance is based on the dynamic moment capacity using empirical equations from ACI 318-14ACI Committee 318, Building Code Requirements for Structural Concrete (ACI 318-14) and Commentary (ACI 318-14R), Farmington Hills, Michigan, 2014. to determine the stress in the prestressing strands at ultimate capacity. This method is used by both USACE PDC and ASCE 59-11 standards, and referred to as "USACE PDC/ASCE Standards" herein. The initial stiffness is based on the average between the gross and cracked moments of inertia, following the guidelines of PDC TR-06-01.

Unlike conventional reinforcement, prestressing strands do not have a well-defined yield point. The analysis of prestressed components therefore requires determining the stress in the prestressing strand, f_{ps}, at the ultimate moment. ACI 318-14 provides an empirical equation (Equation 4) for finding f_{ps}. This is the same method used in current blast documents for prestressed members, adjusted for dynamic material properties.

Equation (4)

where f_{pu} is the specified ultimate stress of the prestressing strand, γ_p is a prestressing type factor (0.28 for low-relaxation strands), β_1 is the stress-block factor, ρ_p is the prestressing reinforcement ratio, and d_p is the depth of the prestressing strands.

Using the prestressing force, the dynamic moment capacity, including axial effects, can be calculated using Equation 5. Note that the axial load is assumed to act through the mid-thickness (t/2) of the cross-section. The depth of the compression block is calculated using Equation 6.

Equation (5)

Equation (6)

The elastic stiffness is based on the average of the concrete gross, I_g, and cracked, I_{cr}, (Equation 7) moment of inertias. The modular ratio, n, is the ratio of steel to concrete modulus of elasticity, and defined in the PCI Design Handbook as:

Equation (7)

While simplified elastic-perfectly-plastic resistance functions are commonly used in blast analysis, BakerRisk developed a more refined resistance function using a moment-curvature model. This model incorporates engineering stress-strain curves to model the concrete and steel material properties and discretizing a cross-section into horizontal strips to calculate the strain at each strip of concrete and layer of steel. Full details of this model are provided elsewhere.Mander, T.J., Lowak, M.J., and Polcyn, M.A. (2016). "Blast Performance of Load-Bearing and Non-Load-Bearing Prestressed Concrete Panels," 2016 PCI Convention and

National Bridge Conference, Nashville, TN. This approach provides indication of the quantitative damage (concrete cracking and crushing, steel yielding etc.) that a panel exhibits under increasing lateral deflection. A comparison of moment-curvature and elastic-perfectly-plastic resistance curves for a load-bearing prestressed concrete panel is shown in Figure 3.

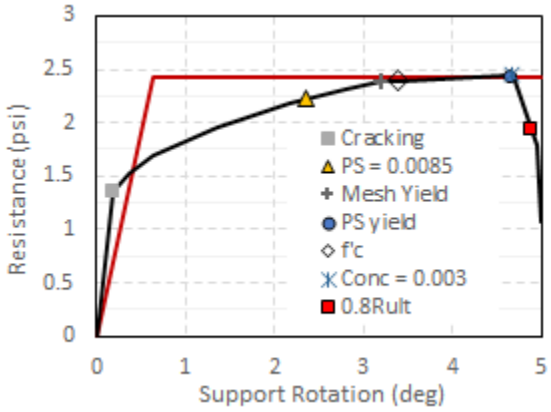

Figure 3. Comparison of Resistance Functions for a Solid Prestressed LB Panel

The resistance functions and blast performance of insulated prestressed non-load-bearing panels have been studied by others.Cramsey, N., and Naito, C., "Analytical Assessment of the Blast Resistance of Precast, Prestressed Concrete Components," Air Force Research Laboratory (AFRL), Technical Report AFRL-ML-TY-TP-2007-4529, Apr. 2007. Naito, C., Hoemann, J., Bewick, B.T., and Hammons, M.I. (2009). "Evaluation of Shear Tie Connectors for Use in Insulated Concrete Insulated Panels," AFRL, Technical Report AFRL-RX-TY-TR-2009-4600, Dec. 2009. Researchers have found that the degree of composite action, with respect to stiffness and strength, is highly dependent on the type of shear connector used. In this research, the steel truss connector was modeled using SAP2000 and LS-DYNA finite element software to quantify the level of composite action achieved. It was found that the resistance values for an elastic-perfectly-plastic system could be approximated by multiplying the ultimate resistance by the ratio of the wythe connector shear capacity over the maximum inter-wythe force.

Using the SDOF models aforementioned, analytical predictions of the shock tube tests were completed. The measured pressure time history was used as the forcing function in the SDOF calculations. The axial load was held constant in the analyses. Shock tube testing showed transient variations in axial load less than 10% of the initial applied loading in panels that did not fail. Table 7 provides the analytical results, comparing the predicted peak displacements and corresponding support rotations for undamaged panels to the experimental results. Ratios of predicted-to-experimental support rotations are plotted in Figure 4 for the undamaged tests using the SDOF moment-curvature and elastic-plastic resistance functions.

Table 7. SDOF Predictions for Undamaged Panels Tested

Test	Axial (kips)	Experimental Displacements (inches)		Analytical Displacements (inches)			
				Moment-Curvature		PDC/ASCE	
		Δ_{max}	θ_{max}	Δ_{max}	θ_{max}	Δ_{max}	θ_{max}
6-inch Solid Prestressed Panel: (5)-⅜" GR 270 Strands Concentric							
1	0	1.8	1.1˚	1.8	1.1˚	1.7	1.0˚
10	144	2.3	1.4˚	2.3	1.4˚	2	1.2˚
15	144	3.4	2.1˚	3.0	1.8˚	2.6	1.6˚
21	88	2.6	1.6˚	2.5	1.5˚	1.9	1.2˚
22	72	3.6	2.2˚	3.3	2.0˚	2.5	1.5˚
27	72	2.75	1.7˚	2.6	1.6˚	1.8	1.1˚
Fully Composite 3/2/3 Insulated Panel: (3)-⅜" GR 270 Strands Concentric each wythe							
5	0	2.3	1.4˚	2.3	1.4˚	2	1.2˚
12	144	Fails ~ 7	---	Fails ~ 5	---	4.4	2.7˚
17	144	1.3	0.8˚	1.2	0.7˚	0.9	0.6˚
23	72	2.0	1.2˚	2.0	1.2˚	2.1	1.3˚
24	72	2.9	1.8˚	2.8	1.7˚	2.8	1.7˚
29	72	3.9	2.4˚	3.8	2.4˚	3.8	2.3˚
Partially Composite 3/2/3 Insulated Panel: (3)-⅜" GR 270 Strands Concentric each wythe							
7	0	1.5	0.9˚	1.4	0.9˚	1.3	0.8˚
13	144	1.5	0.9˚	1.4	0.9˚	1.2	0.7˚
20	144	3.3	2.0˚	Fails ~ 5	---	2.3	1.4˚
25	72	2.4	1.5˚	2.4	1.5˚	2.2	1.4˚
26	72	3.2	2.0˚	3.4	2.1˚	3.1	1.9˚
30	72	5.5	3.4˚	6.1	3.8˚	4.2	2.6˚

In general, the peak displacements predicted using elastic-plastic resistance functions from the PDC/ASCE under-predict the peak displacement. This is attributed to the higher initial stiffness, and lower yield values obtained with an elastic-plastic resistance function compared to the moment-curvature model. Elastic-plastic SDOF models are only intended for undamaged panels; therefore, this method was only used in predicting displacements for undamaged panels.

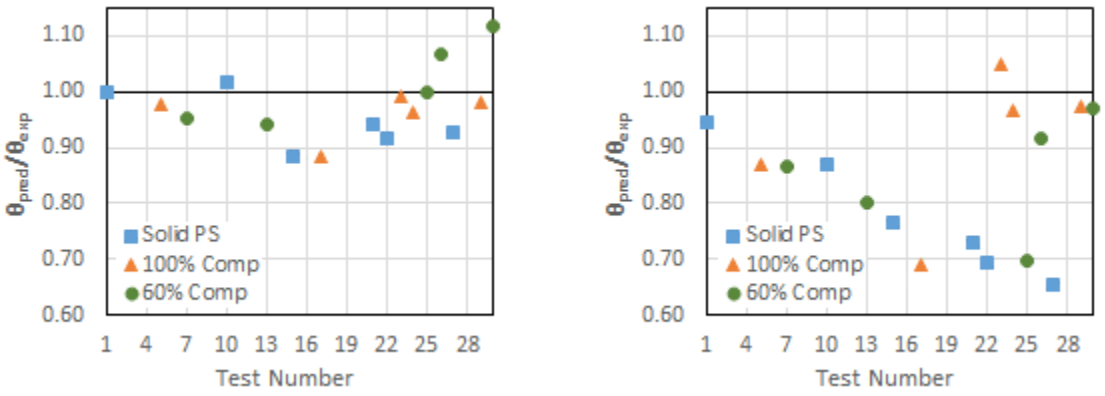

(a) **Moment-Curvature Model** (b) **Elastic-Plastic Model**

Figure 4. SDOF vs. Shock Tube Support Rotations for Undamaged Panels

The moment-curvature model is capable of using modified hysteresis rules that reload at a slope accounting for previous damage. This was done for all thirty tests using the moment-curvature models. Ratios of predicted-to-experimental support rotations are plotted in Figure 5 using the SDOF moment-curvature resistance functions for all tests. Analytical predictions tend to under-predict support rotations with the lowest ratio of 0.88. Nonetheless, the maximum under-prediction difference (Figure 5b) is only 0.25˚, which equates to 0.4 inches over the panel span.

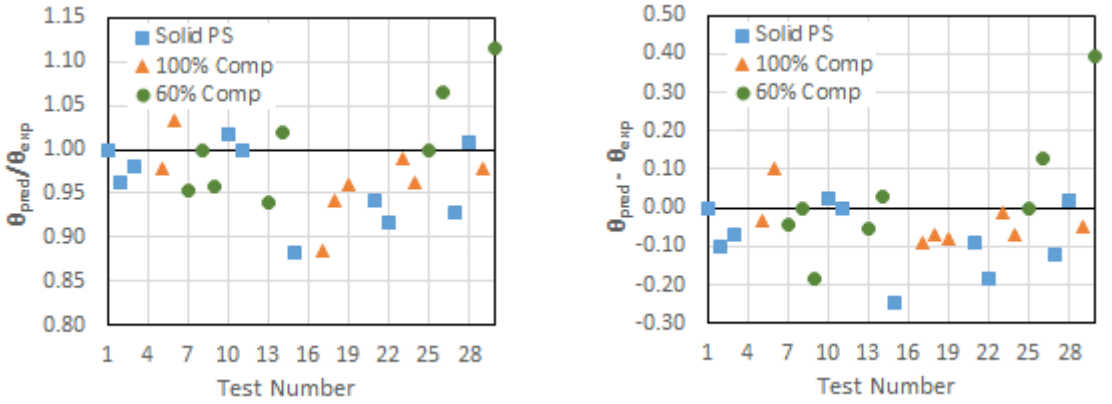

(a) **Ratio of Maximums** (b) **Relative Difference of Maximums**

Figure 5. Moment-Curvature Analytical Comparisons

PROPOSED LOAD-BEARING RESPONSE LIMITS

Blast response criteria are proposed for solid prestressed, and double-wythe prestressed insulated wall panels. Response limits were derived using the analytical moment-curvature models, which were validated with shock tube testing. The analytical models were used in a parametric study to determine response criteria limits suitable for typical prestressed wall construction.

Figure 6 illustrates the process of converting the moment-curvature derived response criteria into criteria that is applicable to elastic-plastic resistance functions. Resistance functions (Figure 6a) are calculated using both methods, and the support rotation limits are calculated for the moment-curvature model (Figure 6b). For each damage threshold, the strain energy, U, is calculated (Figure 6c), and an equivalent support rotation is calculated using the elastic-plastic model by preserving strain energy (Figure 6d).

A parametric study with varying span-to-depth (L/d) ratios, prestressing indexes (ω_{ps}), and axial load ratios (P/f'_cA_g) was completed. For solid prestressed panels, L/d ratios ranged from 48 to 64, which corresponds to 6-inch thick concentrically (d = 3") prestressed panels, 12 feet to 16 feet long. Prestressing indexes ranged from 0.15 to 0.25, which equates to initial effective prestressing values of 250 to 400 psi.

Insulated panels analyzed were limited to 3/2/3 panels (d = 6.5"), assuming fully composite (stiffness and strength) action throughout the panel response. As these members are thicker than solid prestressed panels, the L/d ratios ranged from 26 to 33, or 14-foot to 18-foot spans, respectively. Prestressing indexes were 0.04 to 0.08 which corresponds to initial effective prestressing of 300 to 600 psi. Longer span lengths can be common for prestressed members, but it is demonstrated that higher L/d ratios allow greater support rotations than shorter, thick panels.

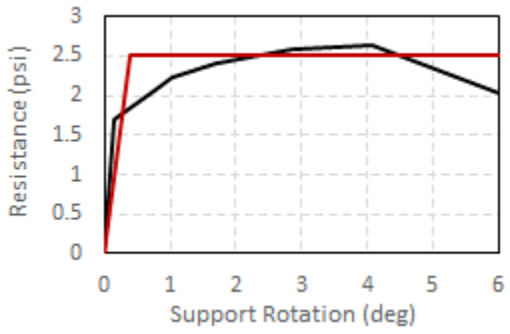

(a) **Compare M-Ø and EP Resistance Functions**

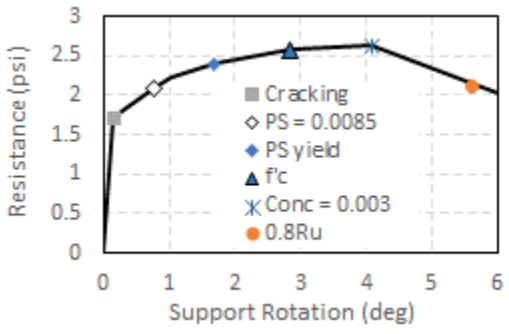

(b) **Determine M-Ø Damage Thresholds**

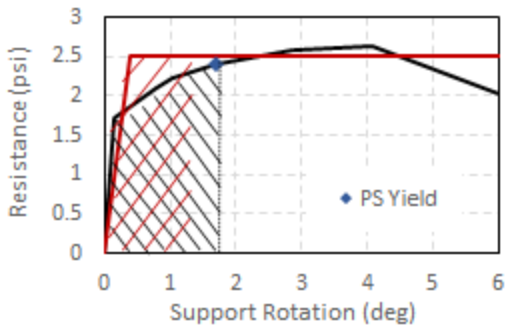

(c) **Calculate Equivalent Strain Energy**

(d) **Convert Calculated Support Rotation to**

EP

Figure 6. Process for Developing Response Criteria for Elastic-Plastic Resistance Functions

Response limits were selected so that a single support rotation for each damage state would satisfy all variations studied. This approach is aligned with the current PDC methodology, which uses a single rotation limit value at each state, irrespective of prestressing index or span-to-length ratio.

LOAD-BEARING SOLID PRESTRESSED PANELS

Axial load levels of $0.05f'_cA_g$ and $0.10f'_cA_g$ were considered for LB solid panels. The same NLB cross-sections were analyzed but with a constant concentric axial load. Limits were set using the same damage states (yielding, crushing etc.), but Heavy and Hazardous support rotations were set as equal. Since a LB failure is a sudden, brittle failure, there is a sudden transition from concrete crushing to complete loss in load-carrying capacity. Proposed response limits are listed in Table 8, using the parametric results of Figure 7. Note that with an axial load of $0.10f'_cA_g$ and prestressing indexes exceeding 0.22, the prestressing steel no longer yields; therefore, lines are not plotted for this case in Figure 7.

Table 8. Proposed Response Limits for Solid Prestressed Wall Panels

Wall Type	Superficial		Moderate		Heavy		Hazardous	
	μ	θ	μ	θ	μ	θ	μ	θ
Load-bearing	1	1°		1.5°		2°		2°

To capture geometric P-delta effects, a ductility limit threshold was set for LB wall components. This limit, given in Equation 8, was derived by including P-delta effects in the moment-curvature resistance function, as shown in Figure 8, and computing the ductility at which the resistance drops to $0.8R_u$. Strain energy was preserved from the moment-curvature analysis from which the ductility limit was calculated using an elastic-perfectly-plastic resistance function. Once this value was computed for multiple prestressing indexes, Equation 8 was best fit to the data. Equation 8 is plotted as a dotted line in prestressed index vs. ductility plots in Figure 9. The span-to-depth ratio was incorporated into this equation to recognize that slender sections are more prone to P-delta failures.

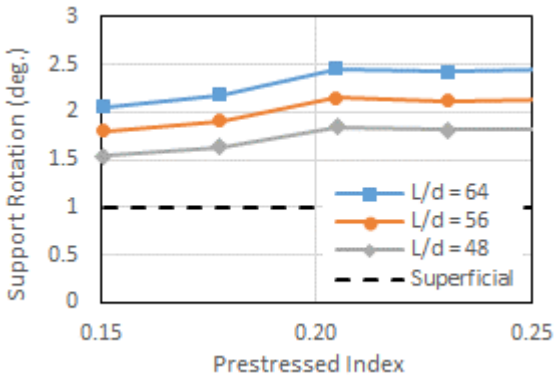

Prestressing Prop. Limit (Axial Load 0.05f'$_c$A$_g$)

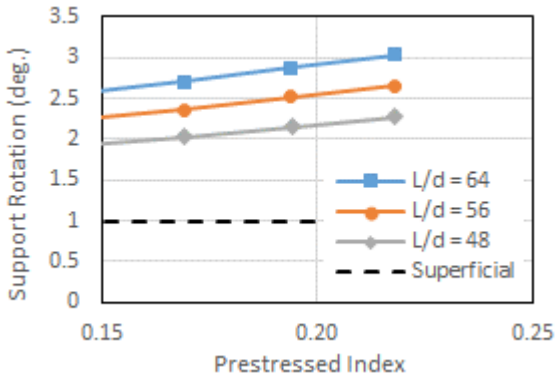

Prestressing Prop. Limit (Axial Load 0.10f'$_c$A$_g$)

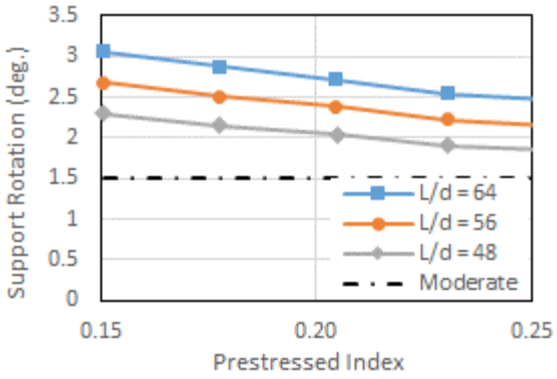

Peak Concrete Stress (Axial Load 0.05f'$_c$A$_g$)

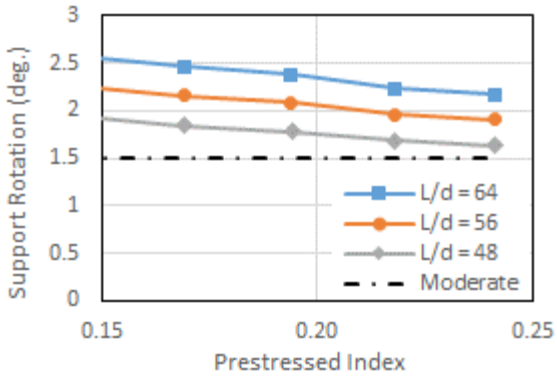

Peak Concrete Stress (Axial Load 0.10f'$_c$A$_g$)

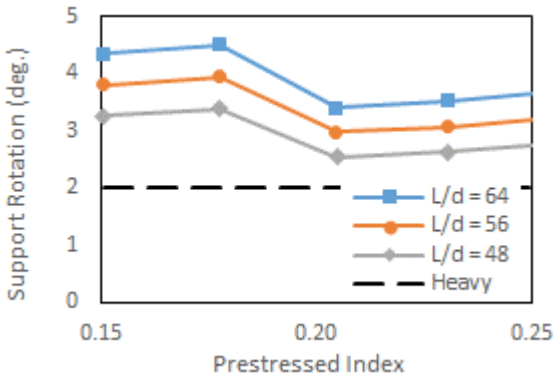

Concrete at 0.003 Strain (Axial Load 0.05f'$_c$A$_g$)

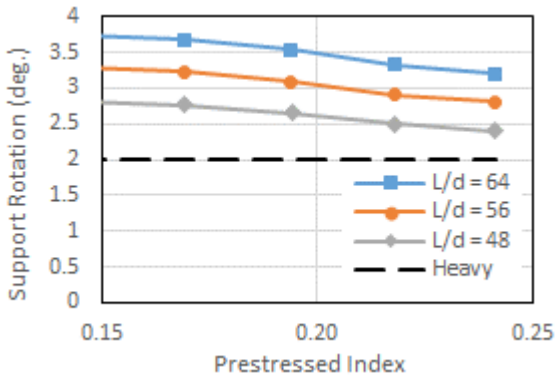

Concrete at 0.003 Strain (Axial Load 0.10f'$_c$A$_g$)

Figure 7. Load-Bearing Solid Prestressed Panel Parametric Study

Equation (8)

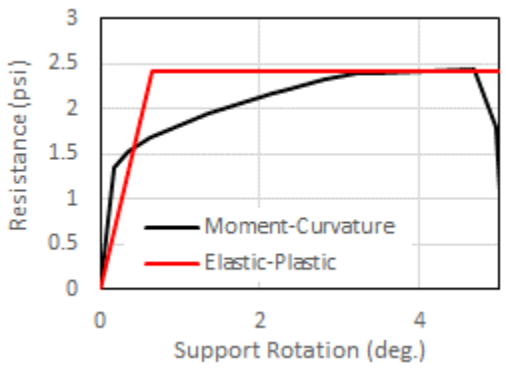

Resistance Function without P-delta Effects

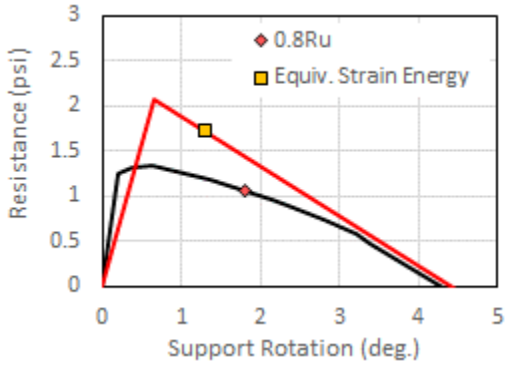

Resistance Function Including P-delta Effects

Figure 8. Determining Failure Limit from P-delta Moment

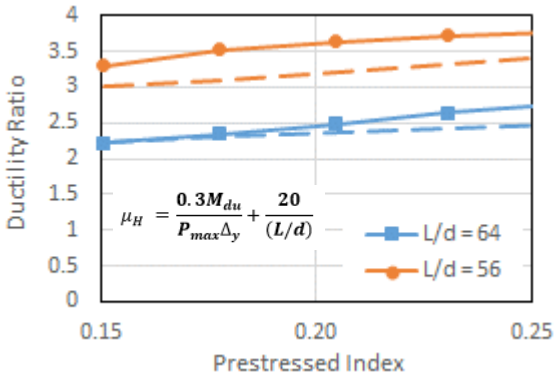

Ductility Equation (Axial Load 0.05f'$_c$A$_g$)

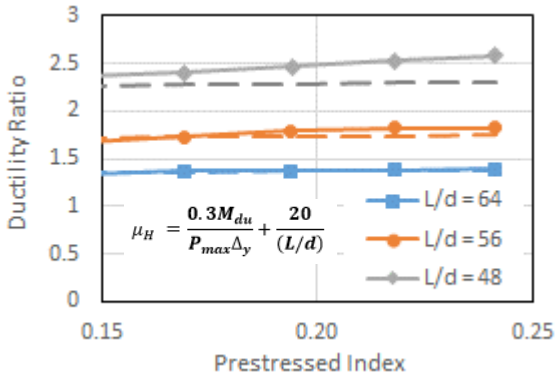

Ductility Equation (Axial Load 0.10f'$_c$A$_g$)

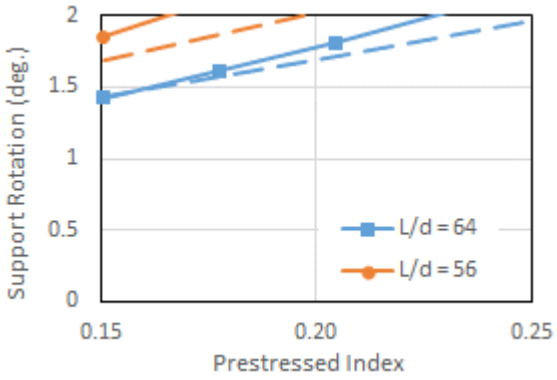

Corresponding Rotation (Axial Load 0.05f'$_c$A$_g$)

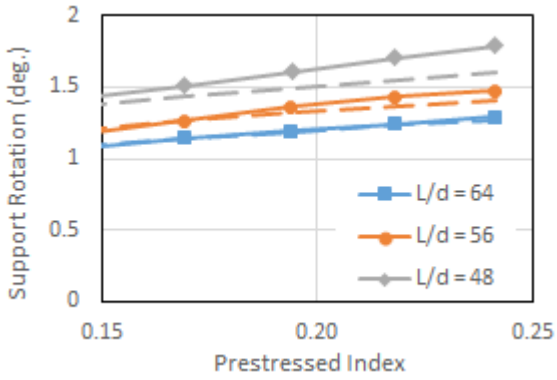

Corresponding Rotation (Axial Load 0.10f'$_c$A$_g$)

Figure 9. Ductility Limit Equation for Solid Prestressed Panel

The ductility equation becomes applicable for walls with axial loads that are significant compared to the moment capacity of a wall in flexure alone. For example, a wall is more susceptible to be governed by P-delta effects when it has a low prestressing index and a long span (low flexural resistance). This is demonstrated in Figure 9. The ductility limit calculated with Equation 8 (dotted lines) was converted to an equivalent support rotation.

Panels with a lower prestressing index and large *L*/*d* ratio have Heavy damage limits to less than 2º: the limit established in Table 8 based on concrete compression strains reaching 0.003. The vertical axes on the support rotation graphs are limited to 2º, as the support rotation limits of Table 8 limits the response to this value.

Fully Composite Prestressed Insulated Panels

Axial load levels of $0.05f'_cA_g$ and $0.10f'_cA_g$ were considered for LB insulated panels. This axial load was assumed to act concentrically with equal magnitude on both wythes. Full composite action (stiffness and strength) were assumed for the analysis. Graphical results of the parametric study are plotted in Figure 10. Proposed response limits are listed in Table 9. Similarly to the solid prestressed criteria, values were selected to apply for most conservative condition. Owing to the fact that the response values are based on peak strains, the proposed limits will be conservative for partially composite panels, such as the partially composite panels tested dynamically in this research.

The influence of the ductility criteria is illustrated in Figure 11, for a fully composite panel with an axial load of $0.10f'_cA_g$. The solid lines represent the ductility at which the resistance drops to $0.8R_u$ and the dotted lines are calculated using Equation 8. Under the parameters considered, the ductility criteria did not control over the support rotation limit for panels with $0.10f'_cA_g$ axial load. The only instance where this equation is slightly unconservative is for very low span-to-depth (*L*/*d*) ratios. As seen in Figure 11, the resistance for *L*/*d* = 26 drops to $0.8R_u$ at just over 1.9°. However, the support rotation requirement of 2° will limit the response within 5% of the displacement at which the resistance drops to $0.8R_u$.

Table 9. Proposed Response Limits for Prestressed Load-Bearing Insulated Wall Panels

Wall Type	Superficial		Moderate		Heavy		Hazardous	
	μ	θ	μ	θ	μ	θ	μ	θ
Load-bearing	1	0.5°		1.5°		2°		2°

The proposed criteria are applicable for simply supported walls that are controlled by flexural failure (adequate shear capacity) and far range blast effects. The limits should be used in conjunction with SDOF resistance functions computed using the PDC TR-06-01 methodology (using elastic-perfectly-plastic resistance functions). For LB panels, the effect of axial load on the compression block depth and increased moment capacity must be accounted for in the resistance function. P-delta effects can be incorporated in the resistance function, or as an equivalent lateral load (Equation 3). The response limits are applicable for static and dynamic axial compression loads. Continuous panels must consider shear-flexure interaction, which were outside of the scope of this research.

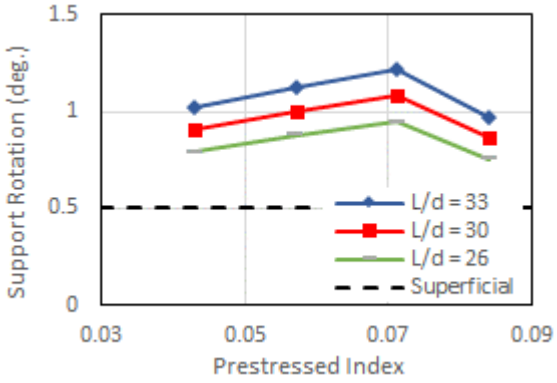

Prestressing Prop. Limit (Axial Load 0.05f'$_c$A$_g$)

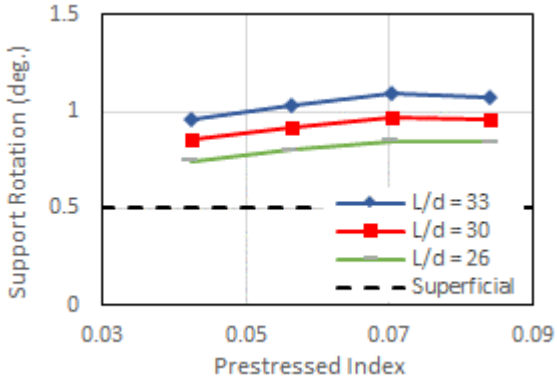

Prestressing Prop. Limit (Axial Load 0.10f'$_c$A$_g$)

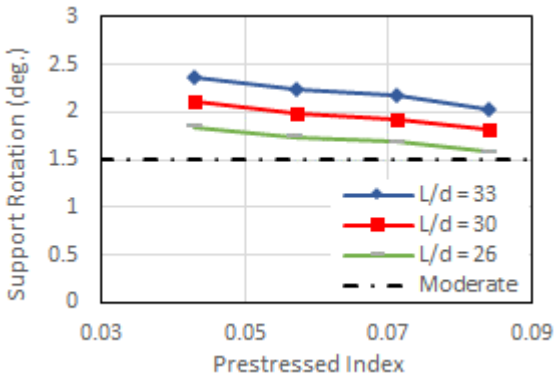

Peak Concrete Stress (Axial Load 0.05f'$_c$A$_g$)

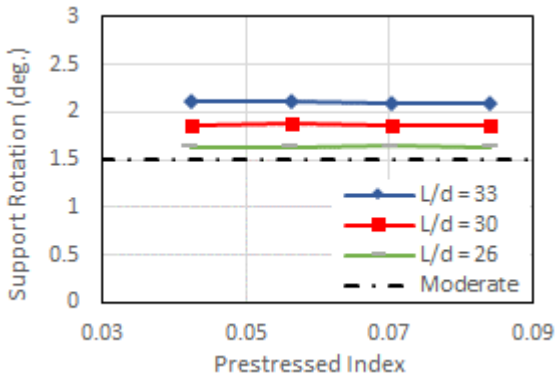

Peak Concrete Stress (Axial Load 0.10f'$_c$A$_g$)

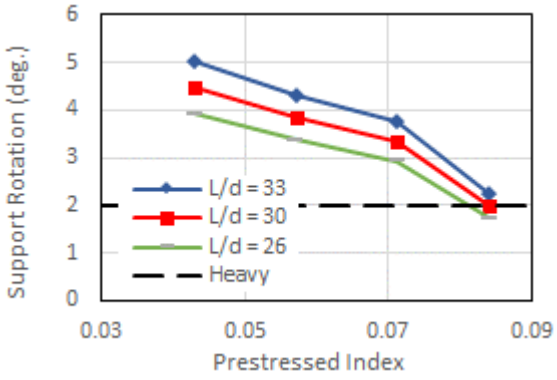

Concrete at 0.003 Strain (Axial Load 0.05f'$_c$A$_g$)

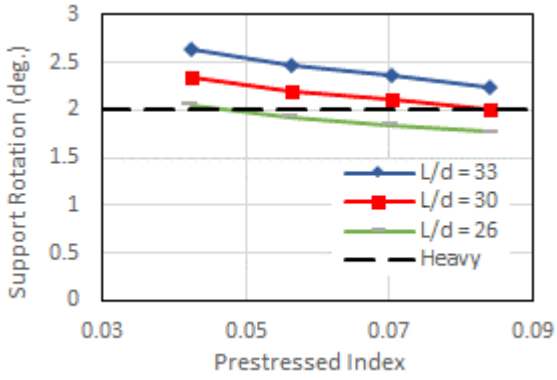

Concrete at 0.003 Strain (Axial Load 0.10f'$_c$A$_g$)

Figure 10. Load-Bearing Fully Composite Insulated Panel Parametric Study

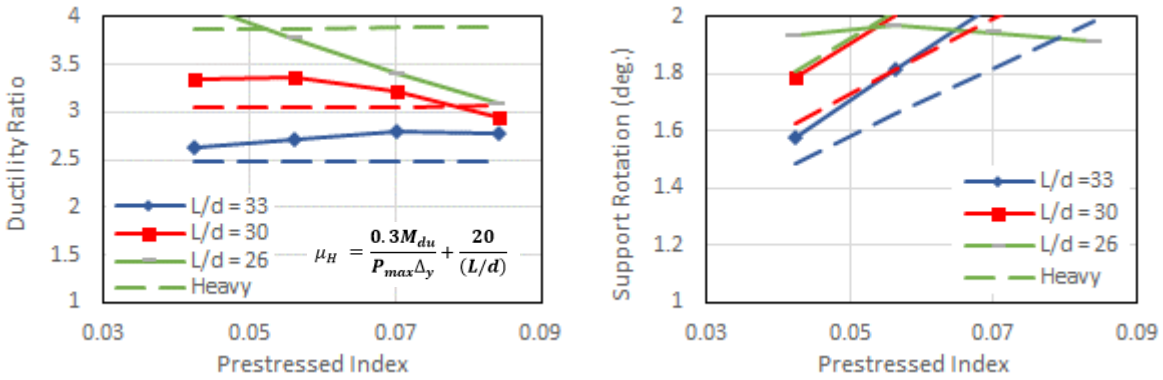

Figure 11. Ductility Limit Equation for Fully Composite Panel with $0.10f'_cA_g$ Axial

CONCLUSIONS AND FUTURE RECOMMENDATIONS

This research studied the blast performance of non-load-bearing and load-bearing prestressed concrete panels both experimentally and analytically. A total of thirty shock tube tests were run on 16-foot tall prestressed wall panels. The walls tested included solid prestressed walls, and fully- and partially-composite walls. LB panels supported static axial loads of $0.05f'_cA_g$ and $0.10f'_cA_g$. These specimens were able to achieve 2º of support rotation without failure. Failure was typically governed by geometric *P*-Δ effects, rather than concrete crushing or strand fracture. This stressed the importance for *P*-Δ effects to be considered in the dynamic response of thin LB elements with low resistances.

A multi-linear resistance function derived through a moment-curvature analysis was developed. This allowed for more accurate predictions of panel displacement than the typically used elastic-plastic idealization. Using the moment-curvature models validated through the shock tube test program, a parametric study was completed to determine appropriate response limits for use with elastic-plastic resistance functions. These limits set a threshold for Moderate damage at 1.5º and Heavy damage at 2º. A ductility term is also introduced to address P-delta failure mechanisms. These limits are only applicable for simply supported walls subjected to a uniform blast load, and not close-in effects. The walls must also be controlled by flexural failure, rather than shear.

FUTURE RESEARCH

The insulated panels that were tested utilized steel truss systems connecting the wythes. It is recognized that a variety of proprietary shear connectors are available to the precast industry. It is recommended that these systems be tested to ensure they satisfy the proposed response limits.

ACKNOWLEDGMENTS

This work was funded by the Precast/Prestressed Concrete Institute. A select advisory committee provided valuable guidance throughout the course of this work, specifically, Roger Becker, Greg Force, Suzanne Aultman, Phil Benshoof, Steven Brock, James Davidson, John Geringer, John Hoemann, Clay Naito and Pat O'Brien. Recognition is also given to Coreslab Structures (Texas) Inc. and Tindall Corporation (Texas) for fabricating and supplying the prestressed wall specimens.

REFERENCES

1. ASCE 59-11, *Blast Protection of Buildings*, Published by the American Society of Engineers (ASCE), Reston, VA, 2011.
2. PDC TR-06-01, "Methodology Manual for the Single-Degree-of-Freedom Blast Effects Design Spreadsheets (SBEDS)," U.S. Army Corps of Engineers (USACE), Protective Design Center (PDC) *Technical Report 06-01*, Sep. 2006.
3. PDC TR-06-08, "Single Degree of Freedom Response Limits for Antiterrorism Design," USACE PDC *Technical Report 06-08*, Jan. 2008.
4. Lowak, M.J., and Montoya, J.R., "Shock Tube Testing of Precast Concrete Panels," Prepared for Protection Engineering Consultants, Inc., *BakerRisk Project No. 01-03471-001-11*, March, 2012.
5. PCI Industry Handbook Committee, *PCI Design Handbook – Precast and Prestressed Concrete,* Seventh Edition, Chicago, Illinois, 2010.
6. Geng, J., Mander, T.J., and Baker, Q.A., "Blast Wave Clearing Behavior for Positive and Negative Phases," *Journal of Loss Prevention in the Process Industries*, available online 24 October 2014.
7. ACI Committee 318, *Building Code Requirements for Structural Concrete (ACI 318-14) and Commentary (ACI 318-14R)*, Farmington Hills, Michigan, 2014.
8. Mander, T.J., Lowak, M.J., and Polcyn, M.A. (2016). "Blast Performance of Load-Bearing and Non-Load-Bearing Prestressed Concrete Panels," *2016 PCI Convention and National Bridge Conference*, Nashville, TN.
9. Cramsey, N., and Naito, C., "Analytical Assessment of the Blast Resistance of Precast, Prestressed Concrete Components," Air Force Research Laboratory (AFRL), *Technical Report AFRL-ML-TY-TP-2007-4529*, Apr. 2007.
10. Newberry, C.M., Davidson, J., Hoemann, J., and Bewick, B.T., "Simulation of Prestressed Concrete Insulated Panels Subjected to Blast Loads," AFRL, *Technical Report AFRL-RX-TY-TP-2010-0014*, Feb. 2010.
11. Davidson, J.S., Newberry, C.M., Hammons, M.I., and Bewick, B.T., "Finite Element Simulation and Assessment of Single-Degree-of-Freedom Prediction Methodology for Insulated Concrete Insulated Panels Subjected to Blast Loads," AFRL, *Technical Report AFRL-RX-TY-TR-2011-0031*, Feb. 2011.
12. Cramsey, N., and Naito, C., "Analytical Assessment of Blast Resistance of Precast, Prestressed Concrete Components," *PCI Journal*, pp. 67-80, Nov-Dec 2007.

13. Naito, C.J., Dinan, R.J., Fisher, J.W., and Hoemann, J.M., "Precast/Prestressed Concrete Experiments – Series 1 (Volume 1)," AFRL, *Technical Report AFRL-RX-TY-TR-2008-4616*, Nov. 2008.
14. Naito, C.J., Hoemann, J.M., Shull, J.S., Saucier, A., Salim, H.A., Bewick, B.T., and Hammons, M.I., "Precast/Prestressed Concrete Experiments Performance on Non-Load Bearing Insulated Wall Panels," AFRL, *Technical Report AFRL-RX-TY-TR-2011-0021*, Jan. 2011.
15. Naito, C., Beacraft, M., and Hoemann, J., "Design Limits for Precast Concrete Insulated Walls Subjected to External Explosions," AFRL, *Technical Report AFRL-RX-TY-TP-2010-0013*, Feb. 2010.
16. Naito, C., Hoemann, J., Bewick, B.T., and Hammons, M.I. (2009). "Evaluation of Shear Tie Connectors for Use in Insulated Concrete Insulated Panels," AFRL, *Technical Report AFRL-RX-TY-TR-2009-4600,* Dec. 2009.